Received: 27 April 2021 | Revised: 23 July 2021 | Accepted: 30 July 2021

DOI: 10.1111/ijac.13857

International Journal of Applied Ceramic Technology

RESEARCH ARTICLE

Fabrication and characterization of Nb_2O_5-doped 3Y-TZP materials sintered by microwave technology

René M. Guillén Pineda[1] | **María D. Salvador**[1] | **Carlos F. Gutiérrez-González**[2] | **Jose M. Catalá-Civera**[3] | **Amparo Borrell**[1]

[1] Instituto de Tecnología de Materiales (ITM), Universitat Politècnica de València, Valencia, Spain

[2] Nanoker Research S.L. Polígono Industrial Olloniego, Oviedo, Spain

[3] Instituto de las Tecnologías de la Información y Comunicaciones (ITACA), Universitat Politècnica de València, Valencia, Spain

Correspondence
René M. Guillén Pineda, Instituto de Tecnología de Materiales (ITM), Universitat Politècnica de València, Camino de Vera, s/n, 46022 Valencia, Spain.
Email: reguipi@upv.es

Funding information
Santiago Grisolía program, Grant/Award Number: GRISOLIAP/2018/168; Ministry of Science, Innovation and Universities (Spain), Grant/Award Numbers: RTI2018-099033-B-C32, RYC-2016-20915

Abstract

The purpose of this research is focused on the manufacture and characterization of a partially stabilized zirconia ceramic with 3 mol% of Yttria and doped with .5 and 1.5 mol% of Nb_2O_5 to analyze the influence of doping, with the purpose of improving the properties before hydrothermal degradation. In the first instance, the microwave sintering process was used for the consolidation of this material, then the physical and mechanical properties were characterized. Together, the results obtained by the conventional sintering process were compared. A low hydrothermal degradation study (LTD) is presented at low temperatures in which possible changes in the mechanical properties of the ceramic materials are analyzed and its influence on the phase transformation that zirconia may present is observed. The mechanical properties were evaluated through hardness, fracture toughness, and Young's modulus tests. Likewise, their density was analyzed, and microstructure was characterized by FESEM. It was found that the microwave-sintered samples at 1200°C exhibited superior properties of toughness than even samples sintered by conventional methods at higher temperatures (1400°C). The sample of 3Y-TZP with 1.5 mol% Nb_2O_5 sintered by microwave with <.2% of porosity achieved a maximum fracture toughness value around 40% higher than the dense monolithic 3Y-TZP material.

KEYWORDS
3Y-TZP, hydrothermal degradation, mechanical properties, microwave sintering, Nb_2O_5

1 | INTRODUCTION

Y-TZP zirconia materials have become increasingly important in recent decades as biomaterials for dental restorations and implants.[1] These materials have excellent mechanical properties, biocompatibility with human tissue, and improved optical properties, making them suitable for extensive commercial application.[2] Regarding the mechanical properties, the values of fracture toughness and hardness are relatively high compared to other bioceramics (4–8 MPa·$m^{1/2}$ and >12 GPa, respectively[3]), and the values of fracture strength range from 900 to 1200 MPa.[4] These values strongly depend on the shape and distribution of the grains as well as the bonding of the interface. However, the main mechanism responsible for its high fracture toughness is the stress-induced phase transformation of the meta-stable tetragonal grains to the monoclinic structure (t–m transformation) around the crack

tip.[5] Nevertheless, this transformation has also become the weakness of this material, as water can spontaneously convert the tetragonal phase to monoclinic when exposed to humid environments.[6] This phenomenon, generally referred to as aging, hydrothermal degradation, or low-temperature degradation (LTD), is accompanied by intergranular microcracking and results in the loss of mechanical properties. In recent years, it has been possible to corroborate the consequences of hydrothermal degradation in applications that work at human body temperature such as hip devices and dental applications.[7]

On the other hand, niobium oxides are presented as a very versatile group of materials because they can give rise to many different and interesting properties.[8,9] Specifically, niobium oxides due to their great potential have been applied as solid electrolytic capacitors, and in many other technological applications as transparent conductive oxides and others. Niobium oxide is a colorless and insoluble solid that is not reactive.[10,11] By combining the excellent properties of both materials, zirconia and niobium oxide, high value-added ceramic composites could be obtained. The development of advanced technologies to produce novel biocompatible materials is motivated, on the one hand, to achieve materials capable of supporting new specifications and applications, and on the other hand, by the increasing industrial demand to manufacture these materials with a low economic cost and a short processing time (<30 min per sample). From the industrial and environment point of view, this means to develop ecofriendly technology to fabricated dense biomaterials.[12,13]

One of the most economical and ecofriendly nonconventional sintering techniques for rapid and homogeneous heating is known as microwave sintering. This technique allows modification of the densification mechanisms through rapid processing and volumetric heating of the material. This heating by electromagnetic microwave radiation depends on the dielectric properties of the material. The consolidation of the ceramic body, as the temperature increases, is due to the activation of the diffusion mechanisms, which forms bridges between the particles, and this phase is known as "necking."[12] Previous studies have shown that it is possible to achieve higher results in the mechanical properties of 3Y-TZP/Nb_2O_5 materials with additions of up to 1.5 mol% of niobium oxide (Nb_2O_5) sintered by conventional method. Kim obtained 3Y-TZP materials containing various amounts of Nb_2O_5 (.5–1.5 mol%) by conventional sintering at 1500°C for 1 h. They claimed that the toughness increased from 6.1 to 11.6 MPa·$m^{1/2}$ with the addition of 1.5 mol% of Nb_2O_5. This increase was produced by the transformation and instability (t → m and m → t phase transformation with temperatures) of 3Y-TZP.[14] The instability causes an increase in the internal stress in the tetragonal lattice caused by decrease of the oxygen vacancies in 3Y-TZP by the doping with Nb_2O_5, responsible for the increases in fracture toughness. Hassan et al. investigated zirconia toughness alumina (ZTA) composites (95 vol.% Al_2O_3) doped with Nb_2O_5 (.2–.6 vol.%) obtained by pressureless sintering at 1500°C up to 1650°C for 1 h. They found that the Vickers hardness and toughness increases with increasing the Nb_2O_5 content.[15] The maximum Vickers hardness of doped ZTA composites was 24.6% higher than undoped ZTA composites. The improvement of Vickers hardness is attributed to the formation of $Nb_2Zr_2O_{17}$ phase that increases the cohesion between the grains; strengthens the phase interface and the grain boundaries of the matrix. The fracture toughness increased from 5.2 to 6.2 MPa·$m^{1/2}$ with the addition of .6 vol.% of Nb_2O_5. Vidyavathy and Kamaraj studied the microwave sintering of 3Y-TZP/Nb_2O_5 in which phase transformation analysis and structural analysis were made to determine changes in the material.[16] In their study, they used a multimode microwave equipment and concluded that combination of transformation toughening and ductile particle reinforcements improved substantially the crack growth resistance and flaw tolerance. Also, the presence of Nb_2O_5 was beneficial to tetragonal to monoclinic transformation and dense, uniform, and fine microstructure was obtained. Decrease in grain size was attributed to fast heating and cooling rate in the case of microwave sintering.

The aim of the present study is to investigate the effect of microwave fast process and correlate the microstructure and mechanical properties of the Nb_2O_5-doped 3Y-TZP at different concentrations (.5 and 1.5 mol%). At the same time, understand the hydrothermal degradation process at different hours of exposition on the 3Y-TZP-Nb_2O_5 ceramics and evaluating the mechanical properties before and after the LTD process and identify possible changes in their phase composition.

2 | MATERIALS AND METHODS

2.1 | Materials processing

The following commercially available powders have been used as raw materials: (a) tetragonal zirconia polycrystals stabilized with 3 mol% Y_2O_3, TZ-3YB-E (Tosoh Corp., Tokyo, Japan), with an average particle size of $d_{50} = .26\,\mu$m; and (b) niobium pentoxide, Nb_2O_5 (Goodfellow, Huntingdon, UK, 99.85% purity). Zirconia and niobium oxide suspensions of 70 wt% solid content were prepared using distilled water as liquid media and 1 wt% addition of an alkali-free organic polyelectrolyte as surfactant (Dolapix CE64). The mixture was homogenized by milling with zirconia balls in polyethylene containers at 150 rpm for 24 h and then dried at 90°C for 12 h. The resulting powder was ground in an agate mortar and subsequently passed through a 75-μm sieve.

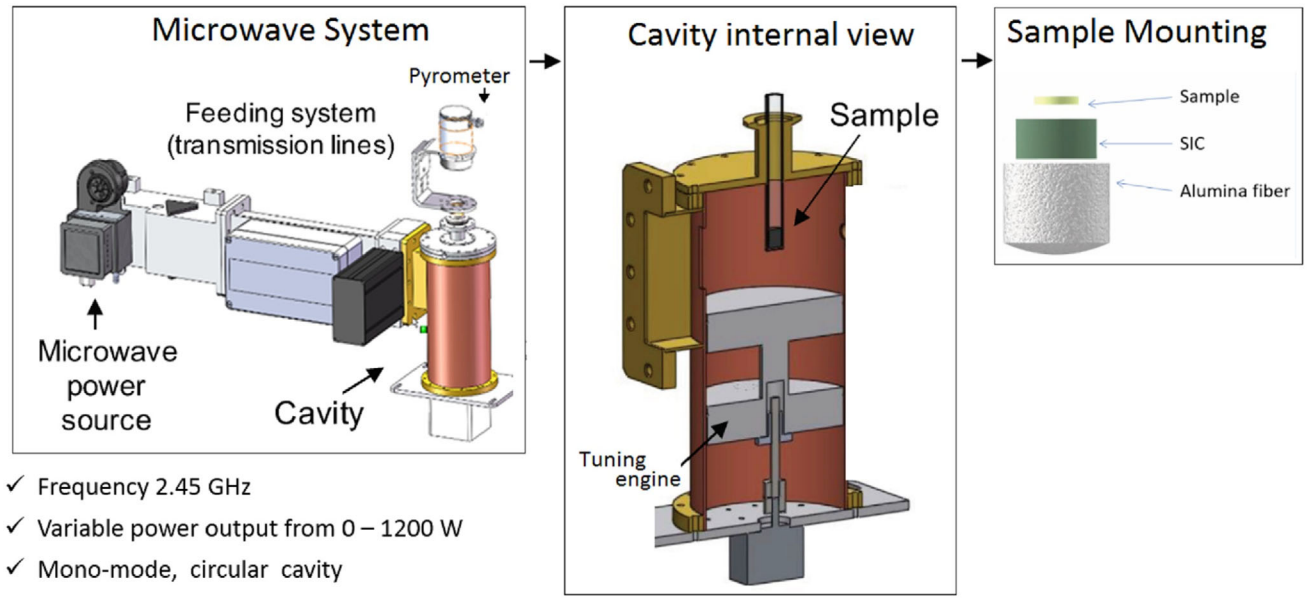

FIGURE 1 Technical parameters, parts, and details of the experimental microwave system of 1 kW at 2.45 GHz connected to a mono-mode circular cavity

For a better analysis of the material, an X-ray distortion analysis was performed on the powdered materials before compaction and sintering to be able to identify the presence of the materials. The samples were measured on a BRUKER Avance A-25 D8 diffractometer. A range of $20° < 2\theta < 70°$, with a step of .03 in 2θ and a measurement time per step of .02 was used for phase identification purposes. The energy dispersive radiation source is of the LYNXEYE type for spot measurements. To carry out a quantifiable analysis of the percentages of each phase, the Toraya method[17] is used. This method makes it possible to obtain the values of the volume fractions of the monoclinic zirconia (m-ZrO_2) and tetragonal (t-ZrO_2) phases, V_m and V_t correspondingly. As indicated by Equation (1), the values of $I_m^{(\bar{1}11)}$, $I_m^{(111)}$ $yI_t^{(101)}$correspond to the characteristic peaks of zirconia in each phase.

$$V_m = \frac{1311\left(I_m^{(\bar{1}11)} + I_m^{(111)}\right)}{1 + 1311\left(I_m^{(\bar{1}11)} + I_m^{(111)} + I_t^{(101)}\right)}. \quad (1)$$

To carry out a quantifiable analysis of the percentages of each phase, the Toraya method is used. This method makes it possible to obtain the values of the volume fractions of the monoclinic zirconia (m-ZrO_2) and tetragonal (t-ZrO_2) phases, V_m and V_t correspondingly.

The obtained powders have been uniaxially compacted at 80 MPa with a Shidmazu AG-X Plus to obtain green samples of 10 mm in diameter and 3 mm in height, which were then employed for the sintering tests.

2.2 | Sintering methods

Specimens were sintered by conventional process (CS) in an electrical furnace Carbolite Gero, HTF 1800 at 1300°C and 1400°C in air with a heating rate of 10°C/min and 2 h of dwelling time. For sintering materials by microwave, a mono-mode circular cavity operating in the TE_{111} mode with a resonant frequency of 2.45 GHz was selected (Figure 1).

This equipment has been designed and manufactured by the ITACA-UPV (Institute of Information and Communication Technologies of the Universitat Politècnica de València (UPV). The *E*-field has a maximum in the center, where the samples are located inside a quartz tube.[18] Due to changes in dielectric constant of the test sample during the sintering process, a movable short circuit located at the bottom of the cavity allows to tune the cavity dynamically.[19] The possibility to tune the cavity also permits to follow a heating slope previously defined by the user to avoid too fast or too slow heating speed. The temperature of the sample is monitored by an infrared radiation pyrometer (Optris CT-Laser GH5, 5 μm), which is focused on the surface sample via the small circular aperture in the wall of the cavity. The emissivity and transmissivity of the material at the final temperature are calculated before sintering test. A silicon carbide susceptor, which acts as a hybrid-heating element, was employed to aid sample heating in the microwave cavity.[20,21] The samples were sintered at 1200°C in air with a heating rate of 100°C/min and 10 min dwelling time at the maximum

temperature. These selected parameters are based on previous studies in our research group where sintering conditions were optimized for zirconia materials.[18–22]

2.3 | Mechanical and microstructural characterization

The bulk density of the sintered samples was measured by Archimedes' principle by immersing the sample into water liquid (ASTM C373-88).[23] Mechanical properties were assessed on surfaces polished down to 1 μm using diamond paste. Hardness (H) and Young's modulus (E) were evaluated via the nanoindentation technique. The system utilized in this work consists of a nanoindenter (G-200; Agilent Technologies, Barcelona, Spain) with a Berkovich tip previously calibrated with silica standard. Tests were performed under maximum depth control of 1500 nm. The contact stiffness was determined by Continuous Stiffness Measurement technique to calculate the profiles of hardness (H) and elastic modulus (E). Each sample was tested with a matrix of 16 indentations, whose amplitude were set to 2 nm at a frequency of 45 Hz. Regarding the fracture toughness values, K_{IC} (MPa·m$^{1/2}$) were calculated by the indentation-fracture method.[24] K_{IC} was measured applying loads of 20 kg for 15 s with a Centaur HD9-45.5 (Metrol Centaur, S.L., Bilbao, Spain).

Microstructures of the specimens were characterized by means of field emission-scanning electron microscopy (FE-SEM, Gemini Ultra 55 model, Zeiss). Thermal etching was performed during 30 min at 100°C below the maximum temperature to reveal grain boundaries. The average grain sizes of zirconia were measured from FE-SEM micrographs by means of the linear intercept method.[25] Approximately 100 grains were considered for each measurement.

2.4 | Characterization of microwave-sintered samples by hydrothermal degradation process (LTD)

The hydrothermal degradation of the 3Y-TZP/Nb_2O_5 material was carried out under conditions that accelerate the aging process. The polished samples with a mirror finish were introduced into an autoclave at a temperature of 120°C and a pressure of 1.3 bar. The characterization of the samples was carried out at 0, 20, 40 and 80 h. The phase analysis was carried out with a micro-Raman spectrometer (LabRam HR UV; HORIBA Jobin Yvon, Longjumeau Cedex, France). Three measurements were made for each of the samples. The range used was 50–900 cm^{-1} with times integration exposure time of 2 min. The laser used was 532 mm.

As shown in Figure 2, there are many proposals for monoclinic phase quantification models using Raman spectroscopy. However, the linear model of Lim et al. has been used, where it represents the monoclinic phase in volume fraction in Equation (2).

$$V_m = \frac{\left(I_m^{(181)} + I_m^{(190)}\right)}{.33\left(I_t^{(147)} + I_t^{(265)}\right) + \left(I_m^{(181)} + I_m^{(190)}\right)}. \quad (2)$$

Based on previous authors such as Muños-Tabares and Anglada, and Presentaet al., this equation offers very low absolute error values compared to the other existing models for quantification of the zirconium monoclinic phase. With the Origin 9 program, the option of peak analysis has been used to identify the intensity values through the calculation by Lorentzian distribution curve.[26,27] A mechanical characterization of the materials was carried out after the study of hydrothermal degradation.

3 | RESULTS AND DISCUSSION

3.1 | Material powder and densification

In Figure 3A, the presence of spherical agglomerated zirconia particles of different sizes can be clearly distinguished. In Figure 3B,C, it is possible to observe the morphology of the starting powders after the milling process by the addition of .5 and 1.5% in moles of Nb_2O_5, respectively.

Applying Equation (1), the volumetric fraction of m-ZrO_2 phases for the powder presents a V_m of 24.70%. It is important to note that the most characteristic peaks corresponding to Nb_2O_5 are overshadowed by those of zirconia between the section of angles $22° < 2\theta < 25°$ and $28° < 2\theta < 30°$. The 3Y-TZP+1.5 mol% Nb_2O_5 powders show its niobium peak at the 22.6° angle (Figure 4).

The density values for all samples sintered via microwave (MW) and CS are shown in Table 1. Theoretical density has been measured from the dense powdered material with a helium pycnometer (AccuPyc 1330, Micromeritics, GA, USA). In a general view, the results show that the sintering processes by MW and CS at different molar concentrations achieve high values of densification around 96% to ~100% of theoretical density. The values indicate that there is a correlation between the Nb_2O_5 content with bulk density of the sintered materials. The increase in the Nb_2O_5 content decreases the bulk density of ceramics, being most outstanding in the samples obtained by CS, thus the relative density of the obtained samples at 1400°C was decreased from 98.6% down to 97.3%, and at 1300°C was decreased from

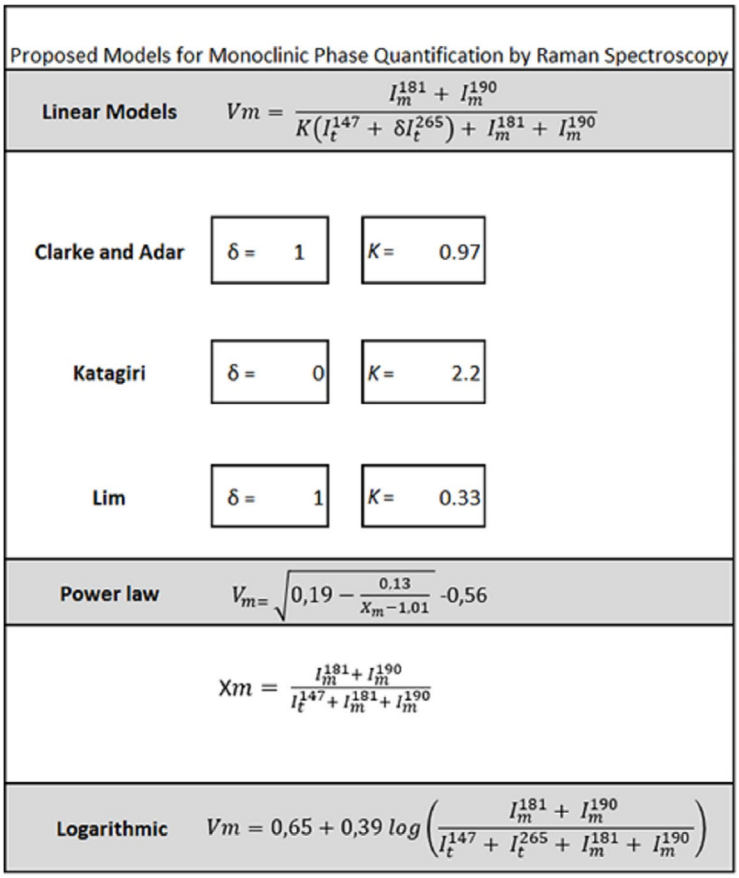

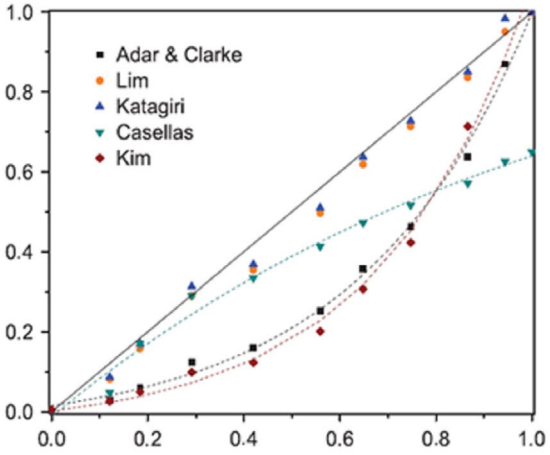

FIGURE 2 Proposed model for monoclinic phase quantification by Raman spectroscopy

TABLE 1 Sintered conditions and density of Nb_2O_5-doped Y-TZP materials at different molar concentrations at microwave (MW) and conventional sintering (CS)

Material	Sintering method	Temperature (°C)	Dwell time (min)	Density (%)
Y-TZP	CS	1300	120	97.9 ± .5
		1400	120	99.5 ± .5
	MW	1200	10	99.4 ± .5
Y-TZP + .5 mol% Nb_2O_5	CS	1300	120	97.2 ± .5
		1400	120	98.6 ± .5
	MW	1200	10	98.8 ± .5
Y-TZP + 1.5 mol% Nb_2O_5	CS	1300	120	96.0 ± .5
		1400	120	97.3 ± .5
	MW	1200	10	98.1 ± .5

97.2% down to 96.0%. When both sintering technologies are compared, the density of Nb_2O_5-doped 3Y-TZP with .5 mol% of Nb_2O_5 samples obtained by MW at 1200°C for 10 min is higher (98.8%) than conventionally processed materials at 1300°C for 2 h (97.2%), despite they were processed with lower temperature and sintering time. When the temperature increases to 1400°C, the samples have the same relative density that samples sintered by MW at 1200°C for 10 min. Briefly, to obtain dense materials with relative densities above >98.5%, it requires 350 min and 1400°C in conventional sintering, whereas the MW needs only 30 min at 1200°C. Therefore, one remarkable result is

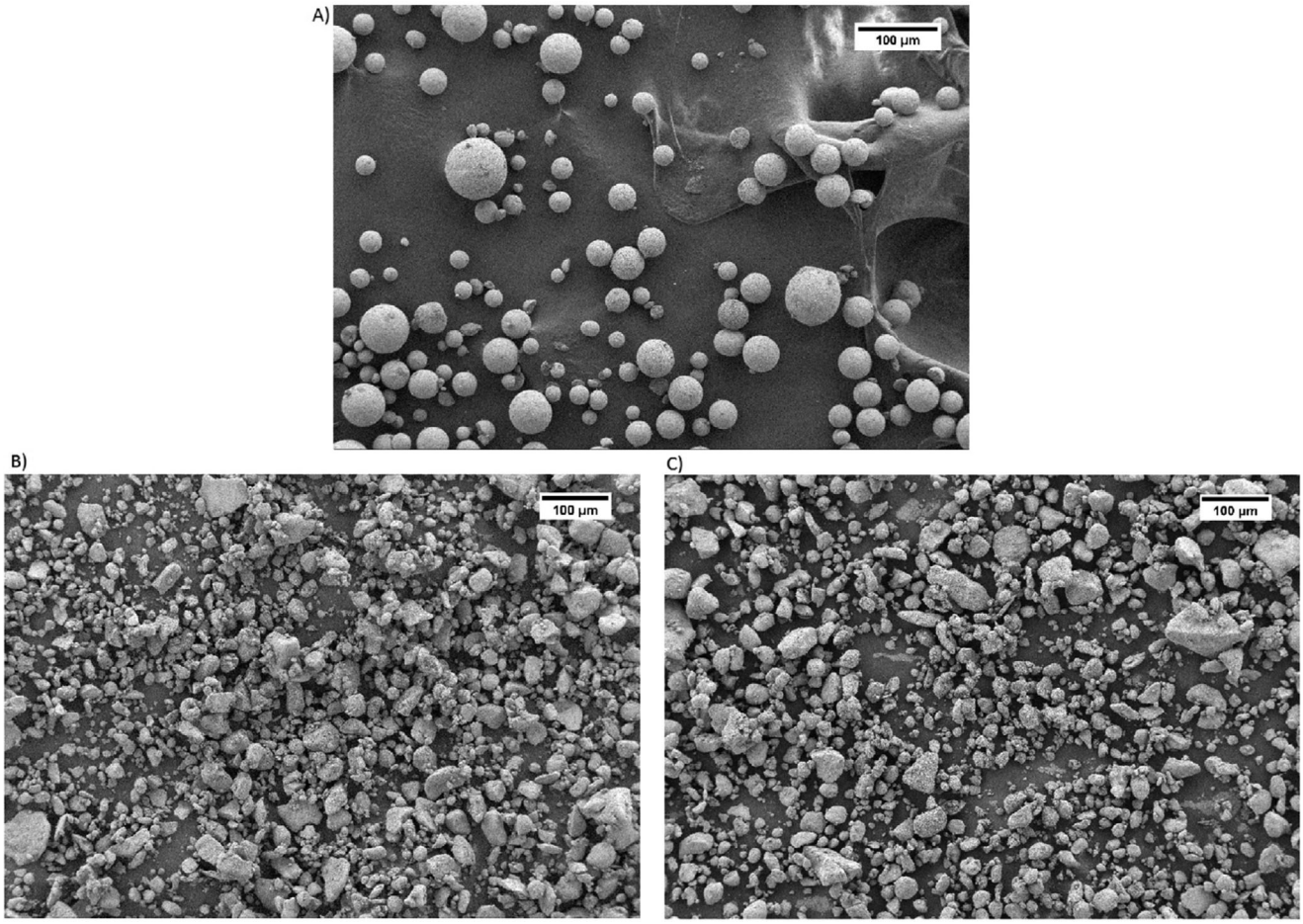

FIGURE 3 Micrograph of the starting powders: (A) 3Y-TZP; (B) 3Y-TZP + .5 mol% Nb_2O_5; (C) 3Y-TZP + 1.5 mol% Nb_2O_5

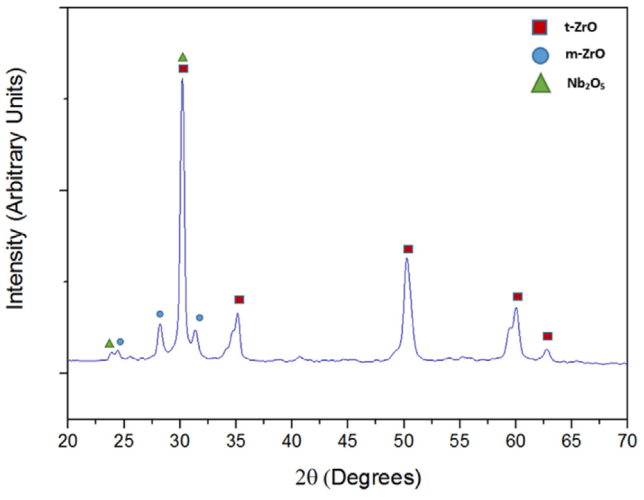

FIGURE 4 X-ray diffraction of the 3Y-TZP + 1.5 mol% Nb_2O_5 starting powders

that microwave sintering allows highly sintered samples to be obtained in less processing time and at considerably lower temperatures than conventional sintering method. It is important to note the high demand for reduced processing times in many fields like the bioceramics sector.

3.2 | Microstructure and grain size

Figures 5 and 6 show representative FE-SEM images of both the reference monolithic ceramic and the materials fabricated in the present study by conventional sintering at 1300°C for 2 h and 1400°C for 2 h, and microwave sintering at 1200°C for 10 min, respectively. There are evident microstructural differences between them.

The samples sintered at 1300°C by CS show a residual porosity and the samples obtained at 1400°C are highly dense. The samples of Nb_2O_5-doped 3Y-TZP at different concentrations and sintered by CS was possible to discern that the grain size of the microstructure is larger than the grain size of the reference material (3Y-TZP). At the same time, the parameters of temperature and sintering process indicate a vast influence in the grain growth of the material. It is possible to observe that the samples sintered by microwave process show a residual porosity as the

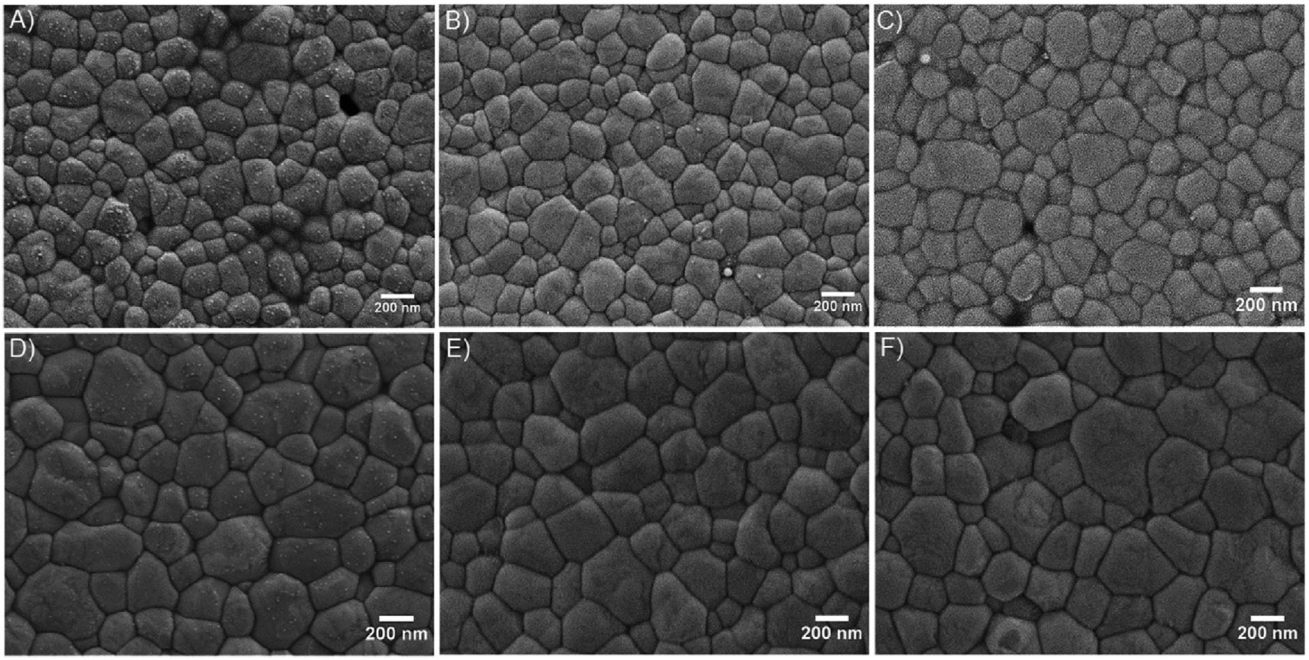

FIGURE 5 FESEM micrographs of (A) reference monolithic 3Y-TZP, and the 3Y-TZP with (B) .5 and (C) 1.5 mol% Nb_2O_5 sintered by conventional method at 1300°C for 2 h. (D) Reference monolithic 3Y-TZP, and 3Y-TZP with (E) .5 and (F) 1.5 mol% Nb_2O_5 sintered by conventional method at 1400°C for 2 h

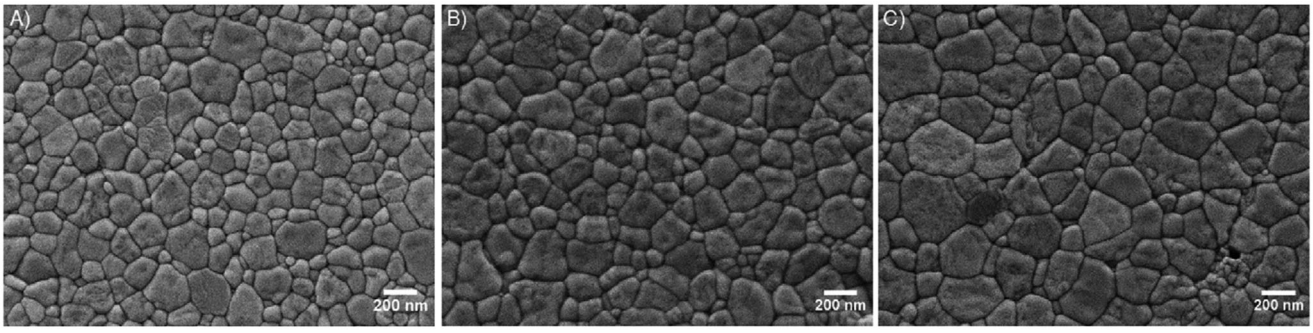

FIGURE 6 FESEM micrographs of (A) reference monolithic 3Y-TZP, and the 3Y-TZP with (B) .5 and (C) 1.5 mol% Nb_2O_5 sintered by microwave method at 1200°C for 10 min

percentage of Nb_2O_5 increase. Figure 7 shows the final grain sizes of zirconia materials, which were measured from their micrographs. It is possible to appreciate the behavior of grain growth by the influence of the doped percentage of Nb_2O_5 at different temperatures and sintering processes. Based on the grain size of the reference material, a tendency of increase in grain size was detected. Therefore, the increase of the content of Nb_2O_5 slightly promoted the grain growth during densification. Nevertheless, it is important to emphasize the value of the grain size of the samples sintered by microwave. Despite of the tendency, the grain size values obtained by MW are lower to those sintered by CS. The average grain sizes of 3Y-TZP and Nb_2O_5-doped 3Y-TZP samples reached approximately 145, 160, and 210 nm, while in CS the values of grain size of 3Y-TZP with 1.5 mol% Nb_2O_5 were 205 nm at 1300°C and 310 nm at 1400°C.

3.3 | Mechanical properties

The mechanical properties, such as Vickers hardness, toughness, and Young's modulus of the materials with different Nb_2O_5 molar concentrations after sintering process, are presented in bar graph in Figures 8, 9, and w10, respectively. The properties were analyzed in the nanoindenter equipment (G-200; Agilent Technologies, Barcelona, Spain) with a Berkovich tip for use on polished surfaces up

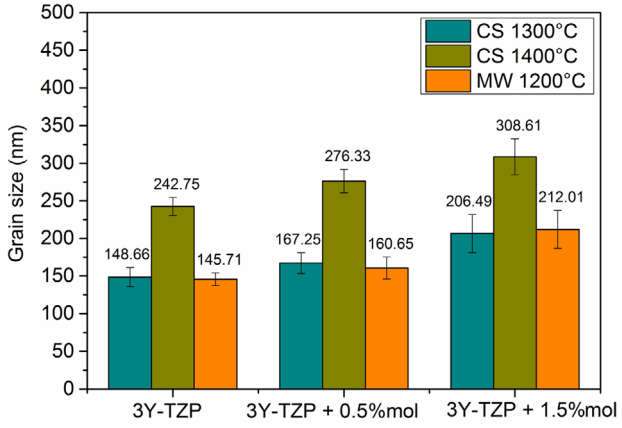

FIGURE 7 Average grain size of 3Y-TZP and Nb_2O_5-doped 3Y-TZP sintered by conventional and microwave process

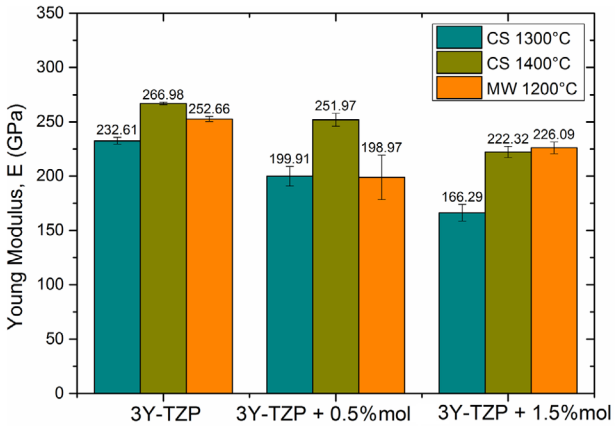

FIGURE 10 Young's modulus values of 3Y-TZP and Nb_2O_5-doped 3Y-TZP with different molar concentrations of Nb_2O_5 after conventional and microwave sintering

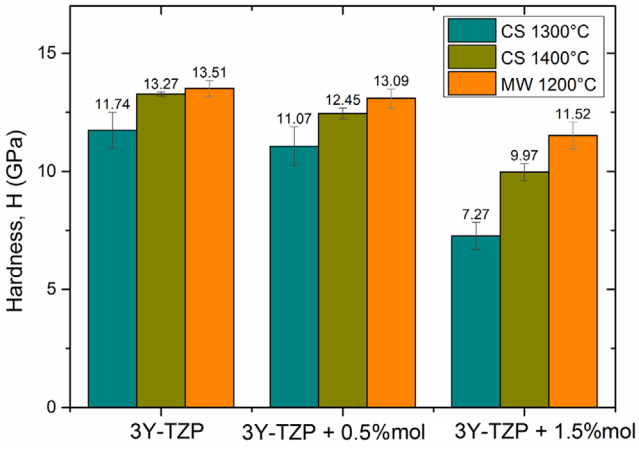

FIGURE 8 Hardness values of 3Y-TZP and Nb_2O_5-doped 3Y-TZP with different molar concentrations of Nb_2O_5 after conventional and microwave sintering

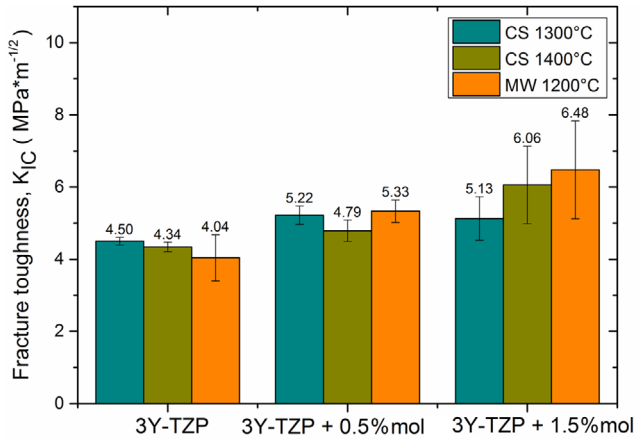

FIGURE 9 Toughness values of 3Y-TZP and Nb_2O_5-doped 3Y-TZP with different molar concentrations of Nb_2O_5 after conventional and microwave sintering

to 1 μm using diamond paste. Figure 8 indicates that the Vickers hardness values tend to decrease with increasing Nb_2O_5 percentage. As can be seen, the materials sintered by conventional sintering at 1400°C show higher values than 1300°C; this is correlated with density values. Comparing sintering method, it is observed that MW samples at 1200°C have greater hardness values than the samples sintered by CS. This is due to the better and faster densification of the MW-sintered specimens and corresponding smaller grain sizes. The best results were obtained with doped samples with .5 mol% of Nb_2O_5 (11.0, 12.4, and 13.0 GPa for CS at 1300°C and 1400°C, and MW at 1200°C, respectively). Regarding doped samples with 1.5 mol% of Nb_2O_5, the hardness increases to 37% when sintering from 1300°C by CS to MW at 1200°C. The authors have not found values of hardness of the Nb_2O_5-doped 3Y-TZP materials sintered by conventional or nonconventional sintering processes reported in the literature so far.

An important observation in Figure 9 is the fact that the sintering process influences the final toughness values, especially in doped samples. The fracture toughness values of the 3Y-TZP + 1.5 mol% Nb_2O_5 materials obtained by conventional sintering at 1300°C and 1400°C, and microwave at 1200°C were 5.1, 6.1, and 6.5 MPa·$m^{1/2}$, respectively. Therefore, the maximum fracture toughness value achieved in the present study was for 3Y-TZP + 1.5 mol% Nb_2O_5 sample sintered by MW at 1200°C. Compared with not-doped 3Y-TZP and doped with .5 mol%, the toughness value increase from 40% to 20%, respectively. Regarding conventional sintered doped materials with 1.5 mol% at 1300°C, the increase corresponds to 21%. This is an excellent value compared with doped and not-doped materials investigated. Therefore, the use of microwave technique is important from the point of view

of fabricated materials along with high fracture toughness values cause a significant reduction of time and energy.

The values of Young's modulus with Nb_2O_5 concentrations are from 166 to 252 GPa (Figure 10). The values decrease simultaneously with Nb_2O_5 concentrations as well as hardness values. High density result in high values of Young's modulus, but this is not a linear relationship. Porosity, grain size, distribution of grains and pores are factors that also affect the values of Young's modulus. By conventional sintering, the highest values were obtained at 1400°C for 3Y-TZP doped with .5 mol% of Nb_2O_5 (252 GPa) according to density values. On the other hand, for higher percentages of Nb_2O_5, the materials obtained at high temperature by CS and MW at 1200°C show similar values between 222 and 226 GPa. These mechanical values correspond to the zirconia values analyzed in previous works of the research group.[20]

This fast-sintering method is a promising process for Nb_2O_5-doped 3Y-TZP materials. The short heating–cooling time of MW (30 min) compared with the long processing time for CS (>12 h) sets important advantages on the industrial application of this method as an advanced process for new technological challenges. An interesting final consideration is that the mechanical and microstructural studies of 3Y-TZP materials with different molar concentrations of Nb_2O_5 have shown the relevance of subtle dependence on the final temperature, Nb_2O_5 content, and sintering technique. Furthermore, the particle size and the distribution of the Nb_2O_5 phase also played an important role in influencing the densification behavior and the mechanical properties. It has been proven that it is possible to obtain 3Y-TZP-doped materials with excellent mechanical properties using the microwave method.

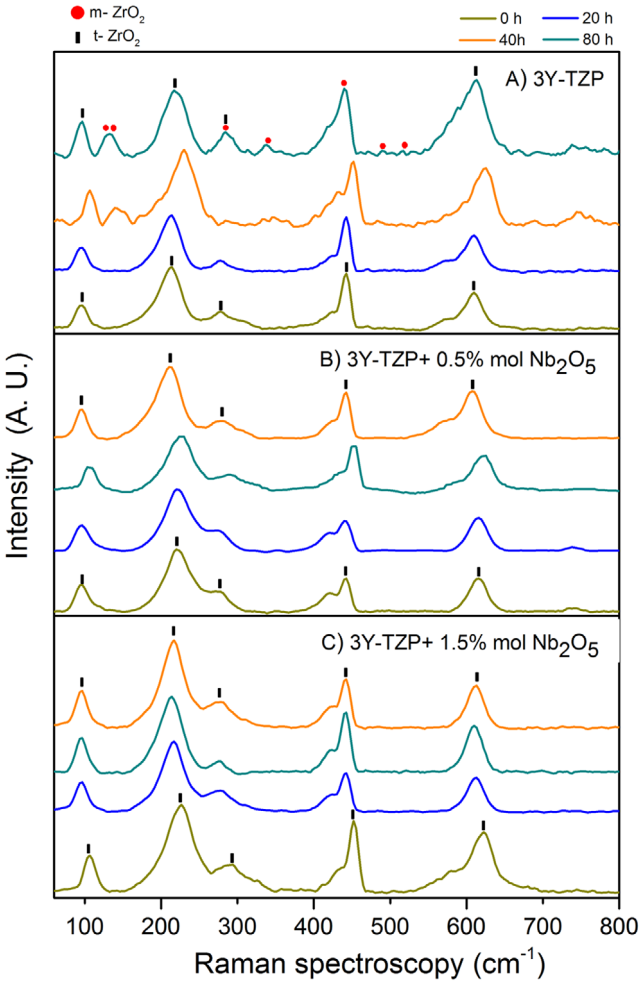

FIGURE 11 Raman spectroscopy of microwave-sintered ceramic materials treated by LTD at different exposure times: (A) 3Y-TZP; (B) 3Y-TZP + .5 mol% Nb_2O_5; and (C) 3Y-TZP + 1.5 mol% Nb_2O_5

3.4 | Hydrothermal degradation (LTD)

As can be seen in Figure 11, a comparison of the results of the Raman spectroscopy carried out on three materials obtained by microwave sintering at 1200°C has been made: (A) 3Y-TZP, (B) 3Y-TZP + .5 mol% Nb_2O_5, and (C) 3Y-TZP + 1.5 mol% Nb_2O_5 after hydrothermal degradation at different exposure times (0, 20, 40, and 80 h). In turn, the comparative graph shows the characteristic peaks of the tetragonal and monoclinic zirconia phases. The graphs with time 0 h of treatment are taken as reference, in which the peaks of the tetragonal phase for each of the materials are identified. At this point, it is detailed that the microwave-sintered materials are not exposed to LTD and do not present any transformation (t → m). When making an exposure at different times of treatment, it can be observed how the characteristic peak of the monoclinic phase is present in the reference material (A) 3Y-TZP, which at 40 h of exposure shows the increase in the range of 170–190 cm^{-1}.

On the other hand, it is possible to notice how the materials (B) 3Y-TZP + .5 mol% Nb_2O_5 and (C) 3Y-TZP + 1.5 mol% Nb_2O_5, when exposed to hydrothermal degradation, do not present any change in their tetragonal phase. In the graphs, the peaks of this phase are very marked and at no time is there any formation of the monocline pass peak, both for the material with .5 and for the one with 1.5 mol% Nb_2O_5, respectively.

Based on the above, Figure 12 shows the evolution of the monoclinic phases in the materials. Based on Equation (2) used to quantify the monoclinic phase of Lim et al., it is only possible to emphasize that the material (A) 3Y-TZP is the one that presents this change and that its percentages change depending on the hours of exposure. As can be seen in the graph, there is a jump in the behavior of the material after 20 h of exposure. These data have been

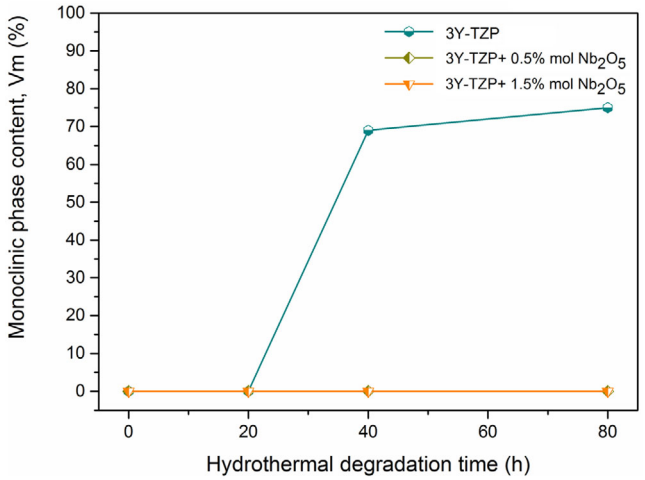

FIGURE 12 Monoclinic phase volume content as a function of hydrothermal degradation exposure time for all samples

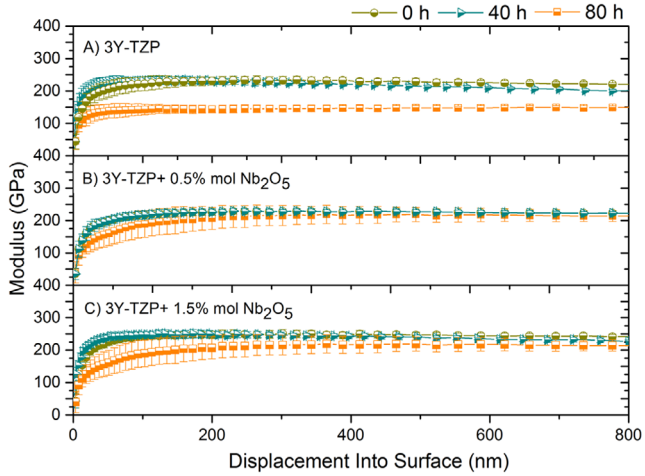

FIGURE 13 Young's modulus as a function of indenter penetration depth profile after LTD for (A) 3Y-TZP, (B) 3YTZP + .5 mol% Nb_2O_5, and (C) 3Y-TZP + 1.5 mol% Nb_2O_5

previously identified in the works previously consulted in the bibliography.[28] For 3Y-TZP, V_m values are increased by increasing LTD. Therefore, based on the formula proposed by Lim et al., making use of the intensity and range values in the spectrum (cm^{-1}), it is possible to obtain the values of the volumetric fraction of the phase. The V_m values for this material are 69% and 75% for 40 and 80 h, respectively.

The mechanical properties have been affected by the exposure to LTD as a function of time, the E and H values have decreased (Figures 13 and 14). This effect is very relevant for the application to which these materials are used (prosthesis and implants). As previously stated, Raman spectroscopy analysis has already shown that materials do not present any transformation in their morphology. However, it is necessary to analyze their behavior when applying a constant load at a given depth. For this, the continuous measurement (CSM) allows us to obtain the new values of hardness and Young's modulus as a function of depth.

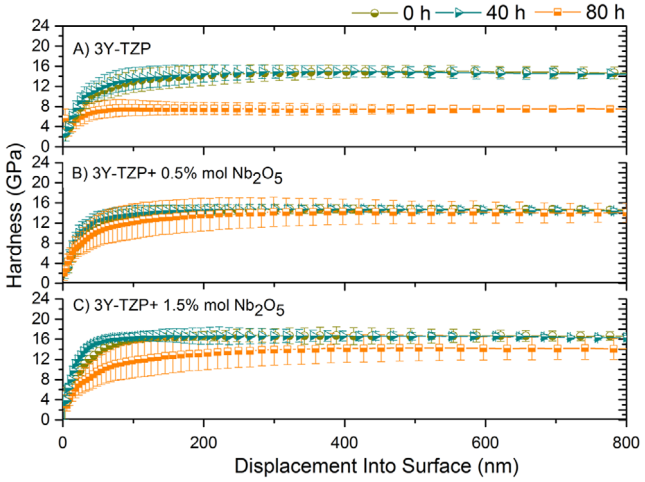

FIGURE 14 Hardness as a function of indenter penetration depth profile after LTD for (A) 3Y-TZP, (B) 3Y-TZP + .5 mol% Nb_2O_5, and (C) 3Y-TZP + 1.5 mol% Nb_2O_5

The Young's modulus values and the hardness values obtained after LTD show a downward trend with respect to the increase in exposure time, whereby the properties decrease. However, in the graphs it is possible to notice that the values at 80 h of degradation are the lowest for each of the cases.

In Figure 13, the data of Young's modulus are shown, in this despite that the materials with niobium oxide do not present much difference between them as the decrease of the properties occurs between 1% and 2%, while the reference material 3Y-TZP shows more notable changes.

The Young's modulus values of 3Y-TZP go from 220 GPa to 0 h. Comparing to 80 h, the values go to 147 GPa, which represents a reduction of 33%. Regarding hardness (Figure 14), the same trend is seen as with Young's modulus. In these data, it is seen how the 3Y-TZP values go from 14 to 7 GPa, having a reduction in hardness of 50%. In the case of niobium oxide materials, there is no identical significant change in hardness values.

4 | CONCLUSIONS

Microwave sintering was found to be beneficial in increasing values of fracture toughness and improved mechanical properties. The grain sizes of microwave-sintered samples are lower than those produced by conventional sintering. The results indicate that the grain sizes of the sintered zirconia were influenced by the addition of Nb_2O_5, the grain

growth is higher with increase in Nb_2O_5 percentages. It can be noticed that microwave sintering at low temperature of 1200°C was most beneficial in enhancing densification and mechanical properties of the ceramic materials. Similarly, the microwave-sintered samples exhibited much superior properties of hardness and toughness even when conventionally samples were sintered at higher temperatures. The Fracture toughness values of 3Y-TZP ceramics with Nb_2O_5 rises with the increase in the Nb_2O_5 content. For this reason, in the sample of 3Y-TZP with 1.5 mol% Nb_2O_5 sintered by MW at 1200°C with <.2% of porosity, it is possible to obtain a maximum fracture toughness value around 40% higher than the dense monolithic 3Y-TZP ceramics. Hydrothermal degradation (LTD) is an important factor in the use of new ceramic materials that have applications in humans. The results demonstrate how the 3Y-TZP/Nb_2O_5 materials influence the absence of a transformation from tetragonal to monoclinic phase. Fabrication of these advanced bioceramics under microwave process at smoother conditions (i.e., at lower temperature to minimize grain growth) without compromising their full densification (using high heating rates) thus emerges as a likely generic economic processing guideline to make them highly mechanically resistant.

ACKNOWLEDGMENTS

The authors are grateful to the Generalitat Valenciana for the funding support for the Santiago Grisolía program (GRISOLIAP/2018/168) and to the Ministry of Science, Innovation and Universities (Spain) through the projects RTI2018-099033-B-C32 (MCIU/AEI/FEDER, UE) and RYC-2016-20915.

CONFLICT OF INTEREST

The authors declare that there is no conflict of interest.

ORCID

René M. Guillén Pineda https://orcid.org/0000-0001-7539-0742
Amparo Borrell https://orcid.org/0000-0003-4292-4538

REFERENCES

1. Piconi C, Maccauro G. Zirconia as a ceramic biomaterial. Biomaterials. 1999;20(1):1–25.
2. Ungureanu DN, Avram D, Angelescu N, Catangiu A, Anghelina FV, Despa V. Comparative study of bioceramic powders synthesis based on calcium and phosphates. Sci Bull Valahia Univ, Mater Mech. 2018;16(14):13–6.
3. Campbell AA. Bioceramics for implant coatings. Mater Today. 2003;6(11):26–30.
4. Adamovic D, Ristic B, Zivic F. Review of existing biomaterials-method of material selection for specific applications in orthopedics. In: Zivic F, Affatato S, Trajanovic M, Schnabelrauch M, Grujovic N, Choy KL, editors. *Biomaterials in clinical practice: advances in clinical research and medical devices*. Cham: Springer International Publishing; 2018. p. 47–99.
5. Guo X. Hydrothermal degradation mechanism of tetragonal zirconia. J Mater Sci. 2001;36(15):3737–44.
6. Gaillard Y, Jiménez-Piqué E, Soldera F, Mücklich F, Anglada M. Quantification of hydrothermal degradation in zirconia by nanoindentation. Acta Mater. 2008;56(16):4206–16.
7. Flinn BD, Raigrodski AJ, Singh A, Mancl LA. Effect of hydrothermal degradation on three types of zirconias for dental application. J Prosthet Dent. 2014;112(6):1377–84.
8. Yoo JE, Park J, Cha G, Choi J. Micro-length anodic porous niobium oxide for lithium-ion thin film battery applications. Thin Solid Films. 2013;531:583–7.
9. Pauline SA, Rajendran N. Biomimetic novel nanoporous niobium oxide coating for orthopaedic applications. Appl Surf Sci. 2014;290:448–57.
10. O'Brien B. Niobium biomaterials. In: Niinomi M, Narushima T, Nakai M, editors. *Advances in metallic biomaterials: tissues, materials and biological reactions*. Berlin, Heidelberg: Springer; 2015. p. 245–72.
11. Nico C, Monteiro T, Graça MPF. Niobium oxides and niobates physical properties: review and prospects. Prog Mater Sci. 2016;80:1–37.
12. Borrell A, Salvador MD. Advanced ceramic materials sintered by microwave technology. In: Liu M, editor. *Sintering technology - method and application*. IntechOpen; 2018. https://doi.org/10.5772/intechopen.78831
13. Gil-Flores L, Salvador MD, Penaranda-Foix FL, Fernández A, Suarez M, Rosa R, et al. Microstructure and mechanical properties of 5.8 GHz microwave-sintered ZrO2/Al2O3 ceramics. Ceram Int. 2019;45(14):18059–64.
14. Kim D-J. Effect of Ta_2O_5, Nb_2O_5, and HfO_2 Alloying on the transformability of Y_2O_3-stabilized tetragonal ZrO_2. J Am Ceram Soc. 1990;73(1):115–20.
15. Hassan AM, Naga SM, Awaad M. Toughening and strengthening of Nb_2O– doped zirconia/alumina (ZTA) composites. Int J Refract Met Hard Mater. 2015;48:338–45.
16. Vidyavathy SM, Kamaraj V. Microwave sintering of niobium co-doped yttria stabilized zirconia. Mod Appl Sci. 2009;3(6):102–5.
17. Toraya H, Yoshimura M, Somiya S. Calibration curve for quantitative analysis of the monoclinic-tetragonal ZrO_2 system by X-ray diffraction. J Am Ceram Soc. 1984;67(6):119–21.
18. Benavente R, Salvador MD, Borrell A, García-Moreno O, Penaranda-Foix FL, Catalá-Civera JM. Microwave, spark plasma and conventional sintering to obtain controlled thermal expansion β-eucryptite materials. Int J Appl Ceram Technol. 2015;12(S2):E187–93.
19. Presenda Á, Salvador MD, Peñaranda-Foix FL, Moreno R, Borrell A. Effect of microwave sintering on microstructure and mechanical properties in Y-TZP materials used for dental applications. Ceram Int. 2015;41(5, Part B):7125–32.
20. Borrell A, Salvador MD, Peñaranda-Foix FL, Cátala-Civera JM. Microwave sintering of zirconia materials: mechanical and microstructural properties. Int J Appl Ceram Technol. 2013;10(2):313–20.
21. Presenda Á, Salvador MD, Moreno R, Borrell A. Hydrothermal degradation behavior of Y-TZP ceramics sintered by nonconventional microwave technology. J Am Ceram Soc. 2015;98(12):3680–9.

22. Borrell A, Salvador MD, Rayón E, Peñaranda-Foix FL. Improvement of microstructural properties of 3Y-TZP materials by conventional and non-conventional sintering techniques. Ceram Int. 2012;38(1):39–43.
23. ASTM C373-14. Standard test method for water absorption, bulk density, apparent porosity, and apparent specific gravity of fired whiteware products, ceramic tiles, and glass tiles. ASTM Int. 2014. https://doi.org/10.1520/C0373-14
24. Kim DJ, Jung HJ, Jang JW, Lee HL, Fracture toughness, ionic conductivity, and low-temperature phase stability of tetragonal zirconia codoped with yttria and niobium oxide. J Am Ceram Soc. 1998;81(9):2309–14.
25. ASTM E112-13. Standard test methods for determining average grain size. ASTM Int. 2013:1–28. https://doi.org/10.1520/E0112-13
26. Lim CS, Finlayson TR, Ninio F, Griffiths JR. In-situ measurement of the stress-induced phase transformations in magnesia-partially-stabilized zirconia using Raman spectroscopy. J Am Ceram Soc. 1992;75(6):1570–3.
27. Muñoz Tabares JA, Anglada MJ. Quantitative analysis of monoclinic phase in 3Y-TZP by Raman spectroscopy. J Am Ceram Soc. 2010;93(6):1790–5.
28. Chevalier J, Gremillard L, Virkar AV, Clarke DR. The tetragonal-monoclinic transformation in zirconia: lessons learned and future trends. J Am Ceram Soc. 2009;92(9):1901–20.

How to cite this article: Guillén Pineda RM, Salvador MD, Gutiérrez-González CF, Catalá-Civera JM, Borrell A. Fabrication and characterization of Nb_2O_5-doped 3Y-TZP materials sintered by microwave technology. Int J Appl Ceram Technol. 2021;**18:**2033–2044. https://doi.org/10.1111/ijac.13857